Journal of Catalysis **211,** 530–539 (2002)
doi:10.1006/jcat.2002.3761

CO Hydrogenation on Ru-Promoted Co/MCM-41 Catalysts

Joongjai Panpranot,* James G. Goodwin, Jr.,*,[1] and Abdelhamid Sayari†

*Department of Chemical Engineering, Clemson University, Clemson, 29634; and †The Center for Catalysis Research and Innovation, Department of Chemistry, University of Ottawa, Ottawa, Ontario, Canada

Received May 28, 2002; revised July 25, 2002; accepted July 30, 2002

A study of CO hydrogenation on MCM-41 and SiO_2-supported Ru-promoted Co catalysts has been performed using both global rate measurements and steady-state isotopic transient kinetic analysis (SSITKA). A significant increase in CO hydrogenation was observed when MCM-41 was used as the support in the order M1 > M2 > SiO_2 at methanation conditions, where M1 and M2 are small pore ($d_p = 3$ nm) and larger pore ($d_p = 7$ nm) MCM-41, respectively. TOF_H based on H_2 chemisorption can be misleading since any suppression of hydrogen chemisorption, as probably occurred for CoRu/M1, results in larger values of TOF_H being calculated. SSITKA results, on the other hand, provide a measure of the "true" intrinsic CO hydrogenation activity of the Co sites. SSITKA studies indicated that the higher CO hydrogenation rates for MCM-41-supported catalysts are due to their greater number of active sites, not to a change in the intrinsic site activity. N_2 physisorption and XRD results reveal that the structure of MCM-41 became less ordered and the surface area decreased after standard reduction and 24 h of FTS, probably due to an effect of water vapor produced during metal reduction and reaction. However, the Co surface was still accessible since there was no significant loss of activity with TOS. The extent of deactivation during the initial reaction period was similar for MCM-41- and SiO_2-supported CoRu catalysts. By providing high activity and unrestricted diffusion of FT reactants and products, CoRu/MCM-41 may be potentially useful for FTS as well as for other catalytic applications, although modified forms of MCM-41 will probably be required in order to increase its hydrothermal stability. © 2002 Elsevier Science (USA)

Key Words: **CO hydrogenation; Fischer–Tropsch synthesis; mesoporous silica; MCM-41; cobalt catalysts; Ru promotion.**

1. INTRODUCTION

Cobalt catalysts are active catalysts for the Fischer–Tropsch synthesis (FTS) of transportation fuels and chemicals from natural gas-derived synthesis gas (CO and H_2) (1–4). Since the catalytically active phase is metallic cobalt, having the cobalt well dispersed and reduced is required for a catalyst to have high activity. High-surface-area supports such as silica and alumina are commonly used as supports for cobalt. In addition to cobalt, a second transition metal, such as Ru (5) Re (6), is often employed in the catalyst in order to increase the reducibility and dispersion of Co. It is well known that Ru-promoted Co catalysts result in higher activity, C_{5+} selectivity, reducibility of Co oxide, and lower coke formation than nonpromoted ones (5, 7–9).

Recently, there have been a considerable number of papers and reviews dealing with the synthesis and characterization of highly uniform mesoporous materials, particularly the hexagonal pore silica-based MCM-41 (10–12). MCM-41 usually has a very high BET surface area, ca. 1000 m^2/g, uniform pore size with average pore dimensions between 1.5 and 10 nm, and high thermal and hydrothermal stability. Use of MCM-41 as a metal catalyst support has resulted in several cases in significant improvements compared to conventional commercial catalysts due to superior dispersion of the active metals (13–15). In a previous study by our group (16), pure silica MCM-41 was synthesized and used as a support for CoRu catalysts. The characteristics of such catalysts in terms of Co dispersion, reducibility, and basic properties for FTS were demonstrated. MCM-41-supported CoRu catalysts were found to have higher activities on a gram catalyst basis for FTS at 220°C and 1 atm than conventional silica-supported ones.

This paper reports CO hydrogenation on MCM-41-supported CoRu catalysts at both methanation and FTS conditions. Steady-state isotopic transient kinetic analysis (SSITKA), developed in large part by Happel (17) and Biloen (18), was utilized to investigate how MCM-41, its pore size, and Co loading affect surface reaction parameters during CO hydrogenation. Time-on-stream behavior was also studied in order to observe the impact of MCM-41 on the initial deactivation process. A conventional amorphous silica-supported Ru-promoted Co catalyst was used as reference material for comparison.

2. EXPERIMENTAL

2.1. Catalyst Preparation

The pure silica MCM-41 employed for this study was prepared in the same manner as that of Kruk *et al.* (19)

[1] To whom correspondence should be addressed. Fax: (864)-656-0784. E-mail: james.goodwin@ces.clemson.edu.

0021-9517/02 $35.00

using the following gel composition: (1.0 SiO_2) : (0.33 TMAOH) : (0.17 NH_4OH) : (17 H_2O), where TMAOH denotes tetramethylammonium hydroxide. Cab-O-Sil silica (40 g, from Cabot Corp.) was mixed manually with 67 g of water. Then, 68.2 g of 25% TMAOH aqueous solution (Aldrich) was added under vigorous magnetic stirring. Another mixture, composed of 40.5 g of cetyltrimethyl ammonium bromide (CTMABr) (Aldrich), 72 g of water, and 13 g of concentrated ammonia (BDH), was prepared during stirring. Both of these mixtures were transferred into a Teflon-lined autoclave, stirred for 30 min, and heated statically at 70°C for 3 days, then at 130°C for 1 day. The obtained solid material was filtered, washed with water, and dried at 60°C. The sample was then calcined in flowing nitrogen up to 550°C (1–2°C/min), followed by calcination in air at 550°C for 5 h. This material is referred to in this paper as small-pore MCM-41 or M1. The larger pore MCM-41, or M2, was prepared by treating the small-pore MCM-41 (before calcination) in an emulsion containing *N,N*-dimethyldecylamine (0.625 g in 37.5 g of water for each gram of MCM-41). The treatment was carried out for 3 days at 120°C. The obtained samples were washed thoroughly, dried, calcined in flowing nitrogen up to 550°C (1–2°C/min), and then calcined in air at 550°C for 5 h. The conventional amorphous silica (SiO_2) was silica grade 952 obtained from Grace–Davison.

The CoRu catalysts were prepared by incipient wetness impregnation of the supports (M1, M2, and SiO_2) using an aqueous solution containing the desired amount of cobalt nitrate (J.T. Baker, Inc.) and ruthenium nitrosyl nitrate (STREM Chemicals). The catalysts were dried overnight in an oven at 120°C and calcined at 300°C in an air flow for 2 h. The M1-supported catalysts were prepared with 5, 8, or 14 wt% Co and 0.5 wt% Ru and are referred to in this paper as 5CoRu/M1, 8CoRu/M1, and 14CoRu/M1, respectively. The M2- and SiO_2-supported catalysts were prepared with 14 wt% Co and 0.5 wt% Ru and are referred to as 14CoRu/M2 and 14CoRu/S, respectively.

2.2. BET Surface Area and Pore Size Distribution

The BET surface area, pore volume, average pore diameter, and pore size distribution of the catalysts were determined by N_2 physisorption using a Micromeritics ASAP 2010 automated system. Each sample was degassed in the Micromeritics ASAP 2010 at 10^{-6} mm Hg and 200°C for 4 h prior to N_2 physisorption.

2.3. XRD Measurements

XRD was performed in order to confirm the structure of MCM-41. A Scintag 2000 X-ray diffractometer with monochromatized Cu $K\alpha$ radiation (40 kV, 40 mA) and a Ge detector was used. The spectra were scanned with a rate of 0.5 degree/min from 1.5–7.0° 2θ.

2.4. Acid Leaching

In order to remove the metals, a 30% hydrochloric acid solution (pH of 1) was used to treat the catalysts for 48 h. After cobalt and ruthenium were dissolved, the residues were filtered and rinsed with deionized water several times to remove all dissolved components. After filtration, the residue was dried under vacuum at room temperature overnight in order to avoid any further reaction caused by heating. The acid-leached catalyst was then characterized.

2.5. H_2 Chemisorption

Static H_2 chemisorption on the reduced cobalt catalyst samples at 100°C was performed using the procedure described by Reuel and Bartholomew (20) with a Micromeritics Chemisorption ASAP 2010 automated system. Prior to H_2 chemisorption, the catalysts were evacuated to 10^{-6} mm Hg at 100°C for 15 min, reduced in flowing H_2 (50 cm^3/min) at 100°C for 15 min, reduced in flowing H_2 at 350°C for 10 h after ramping up at a rate of 1°C/min, and then evacuated at 10^{-6} mm Hg and 350°C for 90 min to desorb any hydrogen. The number of exposed metal atoms on the surface was calculated by extrapolating the total adsorption isotherm to zero pressure and by assuming coverage of one H atom per surface Co^0 atom exposed.

2.6. Temperature Program Reduction (TPR)

The reducibilities of the calcined cobalt catalysts were measured by temperature-programmed reduction using an Altamira AMI-1 system. TPR used a temperature ramp of 5°C/min from 30 to 800°C in a flow of 5% H_2 in Ar. H_2 consumption was measured by analyzing the effluent gas with a thermal conductivity detector. The detector output was calibrated by reduction of Ag_2O powder. The percentage of Co reduced during standard reduction was estimated from TPR at 30–400°C since that has been found to correlate with the reducibility obtained during the optimum standard reduction procedure (reduction at 350°C in flowing H_2 for 10 h after ramping to that temperature at 1°C/min) (21).

2.7. Fischer–Tropsch Synthesis

Fischer–Tropsch synthesis was performed in a downflow differential fixed-bed stainless-steel reactor at 1–2 atm and 220°C. A GHSV of ca. 20,000 h^{-1} and a H_2/CO ratio of 2 were used. The reaction temperature was controlled by a thermocouple inserted into the catalyst bed. The catalyst (ca. 200 mg) was held in the middle of the reactor using quartz wool. It was first heated in a 50 cm^3/min H_2 flow to 350°C, using a ramp rate of 1°C/min, and then reduced *in situ* at this temperature for 10 h prior to reaction. In order to avoid exotherms and hot spots that can lead to rapid catalyst deactivation, reaction was initiated in a controlled manner by gradually increasing the reactant concentrations over a period of 2 h. The final feed flow rate was

$H_2/CO/He = 60:30:10$ (cm^3/min). After the start-up, samples were taken at 3-h intervals and analyzed by GC (Varian CP-3800). Reaction was continued at 220°C for 24 h in order to determine time-on-stream behavior to steady-state reaction.

2.8. Methanation

Rate measurements of methanation were made using ca. 20 mg of the catalyst loaded into the micro quartz flow reactor. The catalyst was pretreated using the standard reduction procedure (heating in 50 cm^3/min H_2 flow to 350°C using a ramp rate of 1°C/min, and then reducing *in situ* at this temperature for 10 h). After reduction, the catalyst bed temperature was lowered to 220°C. The reaction mixture was then introduced to the reactor. The feed consisted of H_2, CO, and He at flow rates of 2, 20, and 8 cm^3/min, respectively. A relatively high H_2/CO ratio was used in order to minimize deactivation due to carbon deposition during the reaction. The total pressure was maintained at 1.82 bar. As the reaction began, reactor effluent samples were taken at 1-h intervals and analyzed by an online GC (Varian CP-3800).

2.9. Steady-State Isotopic Transient Kinetic Analysis (SSITKA) during Methanation

SSITKA is a powerful kinetic technique for studying catalyst surfaces under reaction conditions. This technique was performed as described elsewhere (22). At reaction steady state, transients of methane and CO were obtained by switching the inlet flow of ^{12}CO/Ar to ^{13}CO without disturbing the stability of the reaction. A trace (5%) of Ar in the ^{12}CO was used to account for gas-phase holdup in the system. The decay or increase of isotopically marked species was monitored by an online quadrupole mass spectrometer (Pfeiffer Vacuum). The mass spectrometer was equipped with a high-speed data-acquisition system interfaced to a personal computer using Balzers Quadstar 422 v 6.0 software (Balzers Instruments). Average residence times for the carbon in CH_4 and CO were calculated from these transient studies. The number of surface intermediates, which gave rise to CH_4, and the amount of reversibly chemisorbed CO were also calculated. Information about how SSITKA surface reaction parameters are calculated can be found in a recent review (23).

3. RESULTS AND DISCUSSION

3.1. Characteristics of the Catalysts before FTS

In our study, all catalysts were prepared with Co and Ru to obtain more active catalysts than if they had been prepared with Co alone. The extent of reduction of the bimetallic CoRu catalysts is usually found to be higher than in the corresponding monometallic Co catalysts due to hydrogen spillover from the activation of H_2 on the more easily reduced Ru to cobalt oxide (7–9). Iglesia *et al.* reported that the addition of Ru to Co catalysts not only enhances the catalytic rate, C_{5+} selectivity, reducibility of Co oxide, and stability of Co catalysts, it also decreases the carbon deposition rates during FTS (8, 9). In our study, Co and Ru were assumed to be in intimate contact. There was no evidence that any segregation of the elements occurred after calcination and reduction. Variation in local Ru/Co ratio is possible; however, the amount of Ru used was very low (0.5 wt%) and neither XRD nor EDX was able to effectively detect it.

TABLE 1

Characterization Results (16)

Catalyst	% Co reduced during TPR at 30–400°C[a,b]	Total H_2 chemisorption[a] (μmol H_2/g cat.)	d_p[c] (nm)	% Co[d] dispersion
5CoRu/M1	57	49.1	4.3	12.7
8CoRu/M1	39	54.5	4.5	8.3
14CoRu/M1	38	58.7	7.6	4.8
14CoRu/M2	47	116.1	4.7	9.7
14CoRu/S	58	92.6	7.2	7.7

[a] Error of measurements was ±5%.

[b] Correlates to the percentage of metal reduced during the standard reduction procedure (ramp 1°C/min to 350°C, hold for 10 h) (21).

[c] Based on H_2 chemisorption and the amount of reduced Co from TPR data at 30–400°C, assuming $H/Co_s = 1$ and $d_p = 5/$(metal surface area)/(g reduced Co)/(Co density). Surface area exposed of 1 $Co_s = 6.62$ Å^2.

[d] Based on H_2 chemisorption, assumption of $H/Co_s^0 = 1$, and total amount of cobalt (H/Co_{total}).

Table 1 summarizes the percentage reducibility and H_2 chemisorption for these catalysts (16). For a similar Co loading (14 wt%), the reducibilities during TPR at 30–400°C were found to be in the order 14CoRu/S > 14CoRu/M2 > 14CoRu/M1. The low reducibility of 14CoRu/M1 was suggested to be due to the stronger interaction of Co and M1 due to the effect of higher partial pressure of water vapor developed in the small pore during metal reduction. Water vapor has been reported to facilitate the formation of nonreducible Co-support compounds such as cobalt silicates and cobalt aluminates (21, 24–26). Due to the restricted pore structure of MCM-41, higher partial pressures of water vapor can develop in the pores during reduction. The water vapor effect would be expected to be more pronounced for 14CoRu/M1 than 14CoRu/M2 and 14CoRu/S because of the much smaller average pore diameter of M1. The TPR profiles of such catalysts have been reported (16). More than two major reduction peaks of cobalt oxides were observed and significant reduction was evident above 600°C, suggesting that Co exhibited a stronger interaction with M1 and, thus, manifested a lower reducibility during standard reduction. For 14CoRu/M2 and 14CoRu/S, no reduction peaks above 450°C were observed.

The total amount of hydrogen chemisorbed was found to be in the order 14CoRu/M2 > 14CoRu/S ≫ 14CoRu/M1. The lower H_2 chemisorption for 14CoRu/M1 was probably due in part to its lower reducibility. However, 14CoRu/M2, which also had a lower reducibility than 14CoRu/S, was found to chemisorb more hydrogen than 14CoRu/S. The average Co^0 particle sizes were calculated from H_2 chemisorption results based on the amount of cobalt reduced during TPR at 30–400°C, since this has been found to correlate with the reducibility of the catalyst during the standard reduction procedure (reduction at 350°C in flowing H_2 for 10 h after ramping to that temperature at 1°C/min) (21). The average Co^0 particle sizes did not show any obvious trend; however, the 14CoRu/M2 catalyst exhibited the smallest average Co^0 particle size compared to the other catalysts with similar Co loading. The average Co^0 particle sizes for 14CoRu/M1 and 14CoRu/S were found to be quite similar. The average Co^0 metal particle size for 14CoRu/M1 (7.6 nm) was calculated to be larger than the average pore diameter of the M1 (2.8 nm), suggesting that many larger Co particles may exist on the external surface of M1. A quasi-eggshell-type structure for Co distribution in 14CoRu/M1 granules was apparent from SEM and EDX results (16). Although M1 has a higher BET surface area, it is not as readily available for Co dispersion due to its nonuniform distribution. Overestimation of Co metal particle size is also possible due to particles being occluded in the pores, blocking some of the surface of the particles from adsorbing hydrogen (27), or as a result of H_2 chemisorption suppression. The amount of H_2 chemisorbed and the average Co^0 particle size increased while the reducibility and percentage of Co dispersion decreased with increasing Co loading, from 5 to 14 wt% for the M1-supported catalysts.

3.2. *Fischer–Tropsch Synthesis*

Table 2 presents the Fischer–Tropsch synthesis results at 220°C and 1 and 2 atm pressure. The catalysts with 14 wt% Co and 0.5 wt% Ru were chosen for comparison because of their relatively high activities and their properties closer to those of commercial-type catalysts. Although 14CoRu/M1 had the lowest reducibility and hydrogen chemisorption, it was found to be the most active catalyst for FTS. The order of the activities was found to be 14CoRu/M1 ≈ 14CoRu/M2 > 14CoRu/S. Figure 1 shows the time-on-stream rates (in micromoles of CO converted/gram of catalyst/second) at 2 atm. In general, steady state was reached after 5 h TOS, typical at these conditions. The rates at steady state were about 70–80% of the initial rates. The initial deactivation was probably due to carbon deposition on the active catalyst surface and in the pores. 14CoRu/M1 and 14CoRu/M2, however, maintained their superior activities relative to 14CoRu/S throughout 24 h TOS.

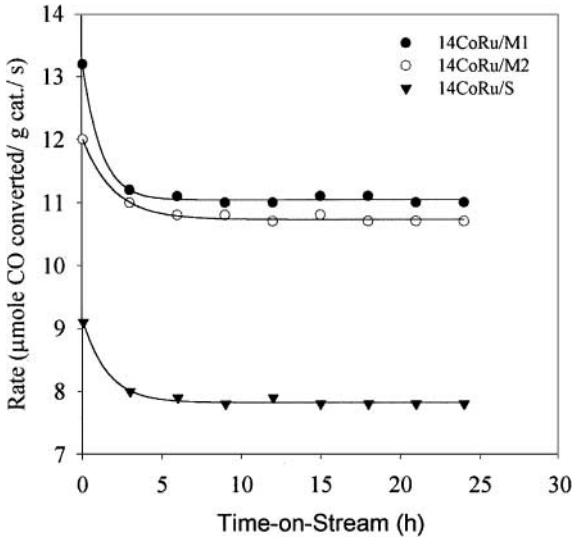

FIG. 1. FTS at 220°C, 2 atm, and $H_2/CO = 2$.

There was an absence of any obvious diffusional effects on product selectivity at the reaction conditions used, since,

TABLE 2

FTS Results[a]

Catalyst	Pressure (atm)	CO conversion[b] (%)		Total Rate[b] (μmol/g cat. s^{-1})		TOF[c] $\times 10^3$ (s^{-1})	Selectivity (wt%)				Chain growth probability (α)	E_{app} kcal/mol or (kJ/mol)
		Initial	Steady state	Initial	Steady state	Steady state	C_1	C_2–C_4	C_5–C_{12}	C_{13+}	(C_5–C_{15})	
14CoRu/M1	1	11.1	7.7	12.4	8.6	73	19.4	46.2	33.8	0.6	0.61	21 (88)
	2	13.2	11	14.7	12.3	105	19.4	46.1	33.9	0.6	0.64	24 (101)
14CoRu/M2	1	10.8	7.2	12.1	8.0	34	19.9	47.3	32.7	0.2	0.57	24 (101)
	2	12.0	10.7	13.4	11.9	51	19.8	47	32.8	0.5	0.62	25 (105)
14CoRu/S	1	6.8	5.8	7.6	6.5	35	18.8	44.5	36.3	0.4	0.60	23 (97)
	2	9.1	7.8	10.2	8.7	47	20.4	48.3	30.7	0.6	0.56	24 (101)

[a] The reaction conditions were 220°C, $H_2/CO = 2$.
[b] Error of measurement was ±5%.
[c] Based on total hydrogen chemisorption.

within experimental error, the activation energies were almost identical for the three different catalysts. This suggests that transport limitations due to the restricted pore structure of the MCM-41 did not appear to be a factor. In the case of 14CoRu/M1, due to Co being concentrated more toward the external surface of the catalyst granules, less reaction might be expected to take place in the interior of the MCM-41 granules. However, for M1-supported catalysts with lower Co loading, Co distribution was more uniform throughout the MCM-41 pores (16). There was no evidence for those catalysts either that reaction on the Co particles inside the pore was limited. If the pores were blocked during reaction so that most/all of the Co surfaces within the pores were inaccessible for reaction, one would expect to have seen a significant loss of activity with TOS. This did not happen to any degree greater than with CoRu/S, as seen in Fig. 1.

The steady-state TOF_Hs for FTS at 1 and 2 atm for 14CoRu/M2 and 14CoRu/S were essentially identical, but that of 14CoRu/M1 was found to be approximately two times higher. Since TOF is calculated based on hydrogen chemisorption before reaction, the low uptake of hydrogen during chemisorption on 14CoRu/M1 resulted in high TOFs being calculated. Given the high reaction rate, it is hard to explain the low amount of hydrogen chemisorbed other than by hydrogen chemisorption suppression. These results call into question the use of traditional hydrogen-based TOFs for drawing any conclusions about reaction on these catalysts.

3.3. Characteristics of the Catalysts after FTS

BET surface areas, pore volumes, and average pore diameters of the catalysts before and after FTS at 220°C and 2 atm are given in Table 3. While BET surface areas and pore volumes of 14CoRu/S and 14CoRu/M2 decreased by ca. 35–40% during FTS, those of 14CoRu/M1 decreased by ca. 70–80%. The average pore diameters for 14CoRu/S and 14CoRu/M2 were not significantly changed during FTS, while that of 14CoRu/M1 increased by ca. 40%. The dramatic decrease in BET surface area and pore volume of 14CoRu/M1 suggested that the pore structure of M1 may be partially collapsed after 24 h FTS or pores may be blocked by F–T products. However, 14CoRu/M1 retained its relative high activity throughout the 24-h TOS, suggesting that the Co surface was still accessible for reaction. Blockage of the pores was, therefore, not likely.

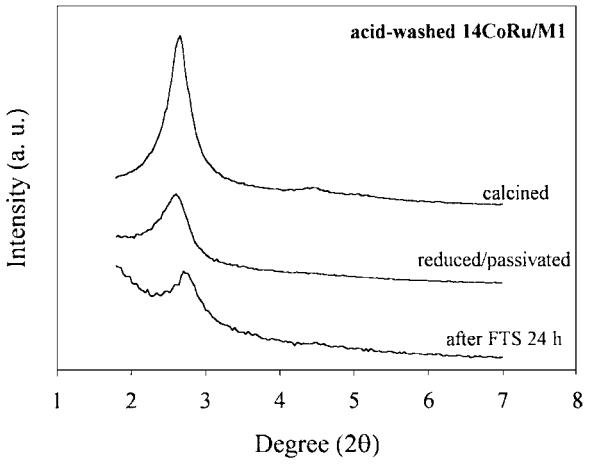

FIG. 2. XRD results of acid-washed 14CoRu/M1.

XRD results for acid-leached 14CoRu/M1 after calcination, reduction, and FTS are displayed in Fig. 2. It was found that after reduction and after 24 h of FTS, the intensity of the [100] MCM-41 reflection peak gradually decreased and the peak became broader. It is suggested that the long range order of the MCM-41 may have partially collapsed during reduction and FTS. This is probably due to an effect of water vapor produced during metal reduction and reaction. The instability of pure silica MCM-41 toward water vapor has also been found by others (28, 29). The partial loss of structural ordering of MCM-41 manifested itself as a significant decrease in pore volume and surface area.

3.4. SSITKA during Methanation

CO hydrogenation at methanation conditions (220°C, 1.8 atm, and $H_2/CO = 10$) was carried out in order to study surface reaction phenomena of the silica- (MCM-41 and SiO_2) supported CoRu catalysts using SSITKA. A relatively high H_2/CO ratio was used in order to minimize deactivation due to carbon deposition during reaction. The

TABLE 3

N_2 Physisorption Results before and after FTS

Catalyst	BET surface area[a] (m^2/g)			Pore volume[a] (cm^3/g)			Avg. pore diameter[a] (nm)	
	Initial	After FTS[b]	% decrease	Initial	After FTS[b]	% decrease	Initial	After FTS[b]
14CoRu/M1	650	122	81	0.34	0.1	71	2.1	3.4
14CoRu/M2	610	358	41	0.62	0.4	35	4.1	4.5
14CoRu/S	219	145	34	1.23	0.78	37	22.6	21.3

[a] Error of measurement was ±5%.

[b] After 48 hours of FTS at 220°C, 2 atm, and $H_2/CO = 2$.

TABLE 4

CO Hydrogenation at Methanation Conditions[a]

Catalyst	Co conversion[b] (%)		Rate[b] (μmol CO/g cat. s^{-1})		TOF_H[c] $\times 10^3$ (s^{-1})	CH_4 selectivity (%)
	Initial	Steady state	Initial	Steady state	Steady state	Steady state
5CoRu/M1	6.2	4.5	4.1	3.1	32	84
8CoRu/M1	15.4	10.1	10.7	7.1	65	84
14CoRu/M1	27.8	17.3	19.4	12	102	84
14CoRu/M2	19.2	13.6	14	9.9	43	83
14CoRu/S	8.2	5	5.7	3.4	18	80

[a] The reaction conditions were 220°C, 1.8 atm, and $H_2/CO = 10$.
[b] Error of measurement was ±5%.
[c] Based on total hydrogen chemisorption.

hydrogenation of CO to form methane has proven to be an ideal system for isotopic transient kinetic investigation due to the simple molecules involved, which are easy to trace by mass spectrometry (30–33). Table 4 presents CO conversions, hydrogenation rates, turnover frequencies, and methane selectivities for these catalysts. For a similar Co loading (14 wt% Co), the catalyst activities were found to be in the order 14CoRu/M1 > 14CoRu/M2 > 14CoRu/S. The methane selectivities of the different catalysts, however, were not significantly different. Figure 3 shows time-on-stream rates for all the catalysts. Steady-state reaction was reached within the first 2 h of TOS for all catalysts. The steady-state rates were ca. 35–45% less than the initial rates for all the catalysts. The steady-state rate for M1-supported CoRu increased by a factor of four when Co loading increased from 5 to 14 wt%. The steady-state rates for 8CoRu/M1 and 14CoRu/M1 were vastly superior to that of 14CoRu/S. 14CoRu/S was found to have a rate similar to 5CoRu/M1. The steady-state TOF_H for 14CoRu/M1 was calculated to be ca. five times higher than that of 14CoRu/S. This result was in the same direction as that observed for CO hydrogenation at FTS conditions ($H_2/CO = 2$), where TOF_H for 14CoRu/M1 was ca. two times greater than that for 14CoRu/S. The TOF_Hs for 14CoRu/M2 and 14CoRu/S, however, were found to be essentially identical. CO hydrogenation is known to be a structure-insensitive reaction (34). Therefore, intrinsic activity would be expected to be constant and independent of dispersion.

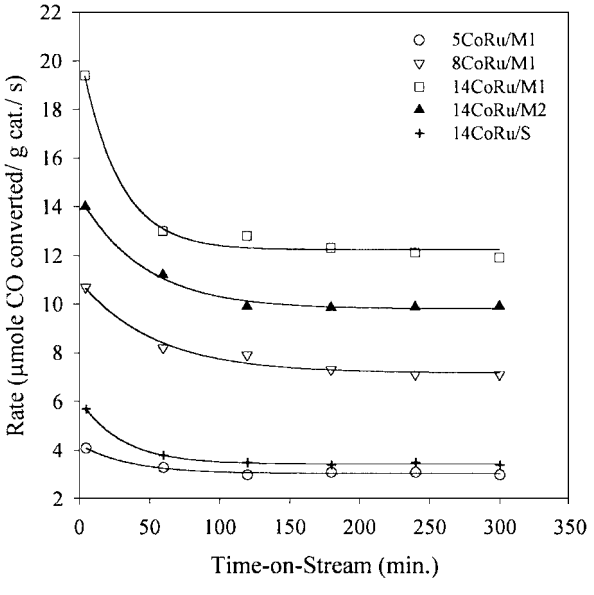

FIG. 3. CO hydrogenation activities at methanation conditions (220°C, 1.8 atm, and $H_2/CO = 10$).

SSITKA of methanation was carried out in order to decouple the contributions to the rate of formation of methane from the concentration of methane intermediates and the average site/intermediate activity. During steady-state reaction, the surface residence times (τ) for CO and CH_4 were determined by integrating the areas between the normalized transient curves for Ar and labeled CO or CH_4, respectively. The pseudo-first-order rate constant (k_M), a measure of intrinsic site activity for methanation, was calculated by taking the inverse of the residence time of CH_4. The surface concentration of methane intermediates, N_M, was determined from

$$N_M = \tau_M \cdot \text{Rate}_{(CH_4)}.$$

The method used to calculate these parameters is described extensively by Shannon and Goodwin (23).

Table 5 gives the SSITKA results for 14CoRu/M1, 14CoRu/M2, and 14CoRu/S. Similar to what was observed for rate of reaction, 14CoRu/M1 and 14CoRu/M2 catalysts had significantly higher concentrations of intermediates leading to methane (N_M) than did 14CoRu/S. No significant variation between the catalysts was observed for the amount of reversibly adsorbed CO (N_{CO}) on the Co surface and its average surface residence time (τ_{CO}). Mesoporous silica supports did not appear to affect the intrinsic methanation activity of the Co sites, since k_M (equal to $1/\tau_M$ and a measure of the "true" TOF for methane formation) was essentially identical for the SiO_2– and the MCM-41-supported

TABLE 5

Surface Reaction Parameters during Steady-State Methanation

Catalyst	Methanation rate[a] (μmol CH_4/g cat. s^{-1})	TOF_H[b] $\times 10^3$ (s^{-1})	τ_{CO}[c] (s)	N_{CO}[d] (μmol/g cat.)	τ_M[c] (s)	N_M[e] (μmol/g cat.)	k_M[f] (s^{-1})	θ_M[g]
14CoRu/M1	10.1	102	1.7	67	4.1	41.3	0.24	0.35
14CoRu/M2	8.2	43	1.5	60	4.2	34.2	0.24	0.18
14CoRu/S	2.7	18	1.4	56	4.4	15	0.23	0.06

[a] The reaction conditions were 220°C, 1.8 atm, and $H_2/CO = 10$. Error of measurement was ±5%.
[b] Based on total H_2 chemisorption and the CO hydrogenation rate.
[c] Error of measurement = ±0.1 s.
[d] Error of measurement = ±3 μmol/g cat.
[e] Error of measurement = ±0.6 μmol/g cat.
[f] $k_M = 1/\tau_M$, pseudo-first-order rate constant.
[g] θ_M is the surface coverage of carbonaceous intermediates, equal to N_M/(total adsorbed H).

Co-based catalysts. The results are in good agreement with the notion that CO hydrogenation on Co is structure insensitive and suggest that there is little support effect on the nature of the active sites.

The observed higher F–T and methanation rates for M1- and M2-supported catalysts can be attributed to an increase in the concentration of active sites. It is known that the number of active intermediates on a Co surface during CO hydrogenation is only a small fraction of the total number of Co metal surface atoms (and hence potential reaction sites) measured by H_2 chemisorption (35). SSITKA results reveal an unexpectedly larger surface coverage of reactive intermediates leading to methane (θ_M) when M1 or M2 was used as the metal support. Surface coverage of intermediates was found to vary in the order 14CoRu/M1 > 14CoRu/M2 ≫ 14CoRu/S. Like TOF_H, surface coverage of reactive intermediates is calculated based on hydrogen chemisorption, and, hence, any suppression of hydrogen chemisorption that might have occurred would result in larger surface coverages being calculated.

For certain catalysts, suppression of H_2 chemisorption has been observed after reduction at certain conditions. For example, reduction of Pt/Al_2O_3 catalysts at or above 773 K has been observed to suppress H_2 chemisorption (36). Metal catalysts supported on SMSI supports or zeolites (37, 38) can also exhibit suppression of H_2 chemisorption, although probably by different mechanisms (39). In this case, low H_2 chemisorption relative to the high reaction rate seen for 14CoRu/M1 is probably due to some sort of Co–MCM-41 interaction. It is difficult to say at this time the exact nature of this metal–support interaction. However, it may be related to the fact that during reduction, because of the smaller pores, there was a higher partial pressure of water vapor. This definitely has an impact on reducibility and may be the cause for H_2 chemisorption suppression at 100°C. The calculated TOF_H and θ_M for 14CoRu/M1, therefore, are probably in error.

Table 6 presents the effect of Co loading on catalyst methanation activities and surface reaction parameters of M1-supported CoRu catalysts. As Co loading increased from 5 to 14 wt%, the methanation rate increased from 2.6 to 10.1 μmol CH_4/g catalyst/s. TOF_Hs based on hydrogen chemisorption also increased, from 0.032 to 0.102 s^{-1}, with increasing Co loading. SSITKA results show that

TABLE 6

Effect of Cobalt Loading on Surface Reaction Parameters during Methanation at Steady State

Catalyst	Methanation rate[a] (μmol CH_4/g cat. s^{-1})	TOF_H[b] $\times 10^3$ (s^{-1})	τ_{CO}[c] (s)	N_{CO}[d] (μmol/g cat.)	τ_M[c] (s)	N_M[e] (μmol/g cat.)	k_M[f] (s^{-1})	θ_M[g]
5CoRu/M1	2.6	32	1.4	55	4.4	11.5	0.23	0.12
8CoRu/M1	6.0	65	1.5	57	4.4	31.0	0.23	0.28
14CoRu/M1	10.1	102	1.7	67	4.1	41.3	0.24	0.35

[a] The reaction conditions were 220°C, 1.8 atm, and $H_2/CO = 10$. Error of measurement was ±5%.
[b] Based on total H_2 chemisorption and the CO hydrogenation rate.
[c] Error of measurement = ±0.1 s.
[d] Error of measurement = ±3 μmol/g cat.
[e] Error of measurement = ±0.6 μmol/g cat.
[f] $k_M = 1/\tau_M$, pseudo-first-order rate constant.
[g] θ_M is the surface coverage of carbonaceous intermediates, equal to N_M/(total adsorbed H).

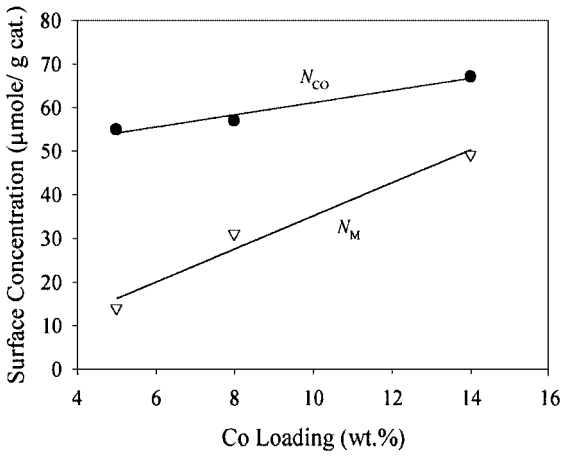

FIG. 4. Effect of Co loading on surface concentrations of reversibly adsorbed CO and of methane intermediates for M1-supported catalysts.

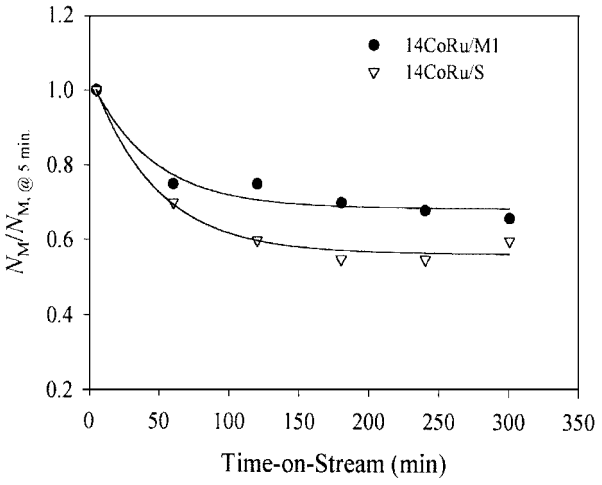

FIG. 5. Effect of time-on-stream on the relative concentration of surface intermediates leading to methane for 14CoRu/M1 and 14CoRu/S.

Co loading had no effect on the intrinsic site activity ($k_M = 1/\tau_M$), since the average surface residence times of the methane intermediates were identical for the different Co loadings. Figure 4 shows the effect of Co loading on the surface concentration of intermediates. The concentration of surface methane intermediates and their surface coverages increased significantly with Co loading. The average surface residence time and the surface concentration of reversibly adsorbed CO slightly increased with increasing Co loading. However, taking into account experimental error and CO readsorption effects, they were not significantly different.

The effect of time-on-stream on specific reaction parameters for 14CoRu/M1 and 14CoRu/S during CO hydrogenation was investigated in order to describe the deactivation of the catalysts from initial reaction to steady state. The steady-state rates were determined to be approximately 55–65% of the initial rate. Effects of time-on-stream on specific reaction parameters for 14CoRu/M1 and 14CoRu/S are reported in Tables 7 and 8, respectively. For both types of silica-supported catalysts, no significant variation in CO adsorption was observed. However, while the average surface reaction residence time of the methane intermediates remained relatively constant, their abundance decreased consistently during the first 50–75 min of reaction. The effect of time-on-stream on the relative concentration of the surface methane intermediates during a TOS of 5 to 300 min for 14CoRu/M1 and 14CoRu/S is shown in Fig. 5. The relative decrease in the number of the surface methane intermediates was found to be 33 and 40% for 14CoRu/M1 and 14CoRu/S, respectively. However, the relative site activity (k_M/k_M, at 5 min) for 14CoRu/M1 and 14CoRu/S was found to stay essentially constant (ca. 0.90). The decrease in the concentration of methane surface intermediates consequently caused the decrease in rate with time-on-stream

TABLE 7

Effect of Time-on-Stream on Surface Reaction Parameters for 14CoRu/M1 during Methanation

Time-on-stream (min)	Methanation rate[a] (μmol CH_4/g cat. s^{-1})	TOF_H[b] $\times 10^3$ (s^{-1})	τ_{CO}[c] (s)	N_{CO}[d] (μmol/g cat.)	τ_M[c] (s)	N_M[e] (μmol/g cat.)	θ_M[f]
5	16.3	165	1.7	68	3.8	62	0.53
30	12.2	124	1.6	62	3.9	48	0.40
50	11.1	112	1.7	68	4.2	47	0.40
75	10.3	105	1.8	71	4.2	43	0.37
120	10.2	103	1.8	71	4.2	43	0.36
300	10.1	102	1.7	67	4.1	41	0.35

[a] The reaction conditions were 220°C, 1.8 atm, and $H_2/CO = 10$. Error of measurement = ±5%.
[b] Based on total H_2 chemisorption and the CO hydrogenation rate.
[c] Error of measurement = ±0.1 s.
[d] Error of measurement = ±3 μmol/g cat.
[e] Error of measurement = ±0.6 μmol/g cat.
[f] θ_M (the surface coverage of methane intermediates) = N_M/(total adsorbed H).

TABLE 8

Effect of Time-on-Stream on Surface Reaction Parameters for 14CoRu/S during Methanation

Time-on-stream (min)	Methanation rate[a] (μmol CH_4/g cat. s^{-1})	TOF_H[b] $\times 10^3$ (s^{-1})	τ_{CO}[c] (s)	N_{CO}[d] (μmol/g cat.)	τ_M[c] (s)	N_M[e] (μmol/g cat.)	θ_M[f]
5	5.0	34	1.5	59	3.9	20	0.11
60	3.2	22	1.4	55	4.3	14	0.07
120	2.9	19	1.4	56	4.1	12	0.06
180	2.7	18	1.4	53	4.0	11	0.06
240	2.7	18	1.3	53	4.0	11	0.06
300	2.7	18	1.4	55	4.4	12	0.06

[a] The reaction conditions were 220°C, 1.8 atm, and $H_2/CO = 10$. Error of measurement = ±5%.
[b] Based on total H_2 chemisorption and the CO hydrogenation rate.
[c] Error of measurement = ±0.1 s.
[d] Error of measurement = ±3 μmol/g cat.
[e] Error of measurement = ±0.6 μmol/g cat.
[e] θ_M (the surface coverage of methane intermediates) = N_M/(total adsorbed H).

and the degrees of deactivation of both catalysts were essentially similar.

4. CONCLUSION

The study presented here shows that potential exists for developing MCM-41-supported CoRu catalysts for CO hydrogenation. Compared to $CoRu/SiO_2$, a marked increase in activity for CO hydrogenation at Fischer–Tropsch and methanation conditions was observed when MCM-41 was used as the metal support for Ru-promoted Co catalysts. The activity was found to vary in the order 14CoRu/M1 (small pore) ≈ 14CoRu/M2 (larger pore) > 14CoRu/S for FTS conditions, and 14CoRu/M1 > 14CoRu/M2 > 14CoRu/S for methanation conditions. SSITKA studies indicated that the increase in CO hydrogenation rate can be attributed to an increase in the concentration of active sites, not to a change in the intrinsic activity. Unrestricted diffusion of reactants and products for CoRu/MCM-41 prepared by conventional incipient wetness impregnation was observed. The extent of deactivation during the initial reaction period was similar on MCM-41- and SiO_2-supported CoRu catalysts. However, as revealed by N_2 physisorption and XRD results, the MCM-41 structure may be partially collapsed due to its instability toward water vapor during catalyst reduction and CO hydrogenation. The calculated values of TOF_H and θ_M based on H_2 chemisorption for CoRu/MCM-41 were probably in error due to some sort of metal–support interaction that led to H_2 chemisorption suppression at 100°C. SSITKA, on the other hand, provided better results for comparing the intrinsic CO hydrogenation activity of the Co sites on the various catalysts.

ACKNOWLEDGMENT

The authors acknowledge the financial support of J.P. by the Royal Thai government.

REFERENCES

1. Anderson, R. B., "The Fischer-Tropsch Synthesis." Academic Press, San Diego, 1984.
2. Eri, S., Goodwin, J. G., Jr., Marcelin, G., and Riis, T., U.S. Patent 4,801,573 (1989).
3. Goodwin, J. G., Jr., *Prep. ACS Div., Petr. Chem.* **36**, 156 (1991).
4. Iglesia, E., *Appl. Catal. A* **161**, 50 (1997).
5. Kogelbauer, A., Goodwin, J. G., Jr., and Oukaci, R., *J. Catal.* **160**, 125 (1996).
6. Hilmen, A. M., Schanke, D., and Holmen, A., *Catal. Lett.* **38**, 146 (1996).
7. Shpiro, E. S., Tkachenko, O. P., Belyatskii, V. N., Rudnyi, Y., Telegina, N. S., Panov, S. Y., Gryaznov, V. M., and Minachev, K. M., *Kinet. Catal.* **31**, 832 (1990).
8. Iglesia, E., Soled, S. L., Fiato, A., and Via, G. H., *J. Catal.* **143**, 345 (1993).
9. Iglesia, E., *Appl. Catal. A* **161**, 59 (1997).
10. Kresge, C. T., Leonowicz, M. E., Roth, W. J., and Vartuli, J. C., U.S. Patent 5,098,684 (1992).
11. Beck, J. S., Vartuli, J. C., Roth, W. J., Leonowicz, M. E., Kresge, C. T., Schmitt, K. D., Chu, C. T., Oslon, D. H., Sheppard, E. W., McCullen, S. B., Higgins, J. B., and Schlemker, J. L., *J. Am. Chem. Soc.* **114**, 10834 (1992).
12. Zhao, X. S., Lu, G. Q., and Miller, G. J., *Ind. Eng. Chem. Res.* **35**, 2075 (1996).
13. Corma, A., Martines, V., and Soria, V., *J. Catal.* **169**, 480 (1997).
14. Song, C., and Reddy, K. M., *Appl. Catal. A* **176**, 1 (1999).
15. Schuth, F., Wingen, A., and Sauer, J., *Microporous Mesoporous Mater.* **44–45**, 465 (2001).
16. Panpranot, J., Goodwin, J. G., Jr., and Sayari, A., *Catal. Today*, in press.
17. Happel, J., *J. Chem. Eng. Sci.* **33**, 1567 (1978).
18. Biloen, P., *J. Mol. Catal.* **21**, 17 (1983).
19. Kruk, M., Jaronice, M., and Sayari, A., *Microporous Mesoporous Mater.* **35–36**, 545 (2000).
20. Reuel, R. C., and Bartholomew, C. H., *J. Catal.* **85**, 78 (1984).
21. Zhang, Y., Wei, D., Hammache, S., and Goodwin, J. G., Jr., *J. Catal.* **188**, 281 (1999).
22. Chen, B., and Goodwin, J. G., Jr., *J. Catal.* **154**, 1 (1995).
23. Shannon, S. L., and Goodwin, J. G., Jr., *Chem. Rev.* **95**, 677 (1995).
24. Kogelbauer, A., Webber, J. C., and Goodwin, J. G., Jr., *Catal. Lett.* **34**, 259 (1995).
25. Backman, L. B., Rautiainen, A., Krause, A. O. I., and Lindblad, M., *Catal. Today* **43**, 11 (1998).

26. Schanke, D., Hilmen, A. M., Bergene, E., Kinnari, K., Rytter, E., Adnanes, E., and Holmen, A., *Catal. Lett.* **34**, 269 (1995).
27. Oukaci, R., Wu, J. C. S., and Goodwin, J. G., Jr., *J. Catal.* **107**, 471 (1987).
28. Ribeiro Carrott, M. M. L., Estevao Candeias, A. J., Carrott, P. J. M., and Unger, K. K., *Langmuir* **15**, 8895 (1995).
29. Kruk, M., Jaroniec, M., and Sayari, A., *Microporous Mesoporous Mater.* **27**, 217 (1999).
30. Winslow, P., and Bell, A. T., *J. Catal.* **86**, 158 (1984).
31. Biloen, P., Helle, J. N., van den Berg, F. G. A., and Sachtler, W. M. H., *J. Catal.* **81**, 450 (1983).
32. Stockwell, D. M., and Bennett, C. O., *J. Catal.* **110**, 354 (1988).
33. Stockwell, D. M., Chung, J. S., and Bennett, C. O., *J. Catal.* **112**, 135 (1988).
34. Boudart, M., and Mariadassou, D., "Kinetics of Heterogeneous Catalytic Reactions." Princeton Univ. Press, Princeton, NJ, 1984.
35. Belambe, A. R., Oukaci, R., and Goodwin, J. G., Jr., *J. Catal.* **166**, 8 (1997).
36. Dautzenberg, F. M., and Wolters, H. B. M., *J. Catal.* **51**, 26 (1978).
37. Gallezot, P., *Catal. Rev.–Sci. Eng.* **20**, 121 (1979).
38. Sayari, A., Wang, H. T., and Goodwin, J. G., Jr., *J. Catal.* **93**, 368 (1985).
39. Oukaci, R., Blackmond, D. G., Sayari, A., Goodwin, J. G., Jr., Stevenson, S. A., Raupp, G. B., Dumesic, J., Tauster, S. J., and Baker, R. T. K., *in* "Metal-Support Interactions in Catalysis, Sintering, and Redispersion" (S. A. Stevenson, J. A. Dumesic, R. T. K. Baker, and E. Ruckenstein, Eds.), p. 112–120. van Nostrand Reinhold, New York, 1987.